

## Estimating Surfactant Surface Coverage and Decomposing its Effect on Drop Deformation

Y.T. Hu and A. Lips

*Unilever Research U.S., 45 River Road, Edgewater, New Jersey 07020, USA*  
(Received 30 January 2003; published 24 July 2003)

A novel method is introduced to estimate surface coverage and the equation of state of insoluble surfactant on droplets, involving measurement of interfacial tension on a single parent drop and progressively subdivided generations of daughter drops. This has enabled quantitative decomposition of the dilution, tip-stretching, and Marangoni effects of surfactants on drop deformation. For a small viscosity ratio of 0.09, the Marangoni effect dominates, increasing first and then decreasing with surface coverage, the dilution effect is significant at high, and tip-stretching only at low surface coverage. For a viscosity ratio of 2.3, the dilution effect dominates, and neither Marangoni nor tip-stretching effects play an important role.

DOI: 10.1103/PhysRevLett.91.044501

PACS numbers: 47.55.Dz, 47.20.Dr

This paper describes how surface coverage of insoluble surface active molecules can be determined by a single drop deformation method. We use this new measurement capability to elucidate how in detail insoluble surfactants influence the Marangoni, dilution, and tip-stretching mechanisms of drop deformation.

The deformation of a liquid drop suspended in an immiscible medium due to an external flow has been the subject of numerous studies since Taylor's pioneering work [1–3]. The major parameter governing the drop deformation is the ratio of the viscous stress and the Laplace pressure, i.e., the capillary number  $Ca \equiv \dot{\gamma} r \eta_s / \sigma$ , where  $\dot{\gamma}$  is the shear rate,  $r$  is the drop radius,  $\eta_s$  is the viscosity of the suspending medium, and  $\sigma$  is the equilibrium interfacial tension. For the same  $Ca$ , the drop deformation slightly increases with the viscosity ratio  $\lambda \equiv \eta_d / \eta_s$ , where  $\eta_d$  is the viscosity of the drop fluid. For the same  $\lambda$ , the deformation increases with  $Ca$ . In real systems, surfactants are often present at the drop surface either as impurities or intentional additives, which inevitably modify the drop deformation from that of a clean drop [4–11]. The obvious effect due to a reduction of the equilibrium interfacial tension can be straightforwardly incorporated into the capillary number. However, there are more mechanisms through which surfactants change the drop deformation, which have been categorized into surface dilution, tip-stretching, and Marangoni effects [12–15]. The increase of the surface area of a drop when it is deformed to a nonspherical shape dilutes the surfactant surface concentration, which increases the interfacial tension and thus decreases the deformation from that expected for the equilibrium  $\sigma$ . This is called the surface dilution effect. Surfactants may accumulate at the tip of the drop due to convection, which decreases the local interfacial tension and causes the tip to be overstretched. This effect is called tip-stretching. The Marangoni stresses arise from the interfacial tension gradient generated by the convection. These stresses retard the surface flow and consequently increase the

deformation. The overall drop deformation at a fixed apparent capillary number depends on the competition of these three effects. Previous experiments and numerical simulation have suggested an intriguing interplay of the three competing effects. The ability to measure surface coverage and three dimensional drop shape enables us for the first time to resolve individual contributions at a quantitative level.

Our model systems consist of several immiscible polymeric liquids. Polydimethylsiloxane (Mn = 117 K, United Chemical) was used as the suspending phase. Polybutadiene (Mn = 5 K, Aldrich) and carboxyl functionalized polybutadiene (Mn = 10 K, Polymer Sources) were used as drop phases. Surfactants were generated at the drop interface by reaction between the carboxyl functionalized polybutadiene and amine functionalized polydimethylsiloxane (Mn = 27 K, United Chemicals). This reaction produces ionic complexes that stay at the interface. More details of the sample preparation can be found elsewhere [7].

Drop deformation experiments were performed in a four-roll mill apparatus with 3D imaging and contouring capabilities as described elsewhere [16]. Drop dimensions were measured using a derivative edge detection algorithm. All experiments were carried out at  $22 \pm 0.2$  °C. Interfacial tension was inferred from the drop deformation using the small deformation theory, which predicts  $D = 2Ca(19\lambda + 16)/(16\lambda + 16)$  [1]. In this equation  $D$  is the deformation parameter defined as  $(L - B)/(L + B)$ , where  $L$  and  $B$  are the drop length and breadth in the flow plane, respectively. We kept the deformation below 0.1 for the interfacial tension measurements. At such small deformation, the change of surface area is typically less than 0.2% and  $\gamma$  can be approximated as the equilibrium value for drops with surfactants.

In order to calculate the magnitude of the surface dilution effect, we first established the dependence of interfacial tension  $\sigma$  on surfactant surface concentration  $\Gamma$  by a novel drop deformation method similar to a

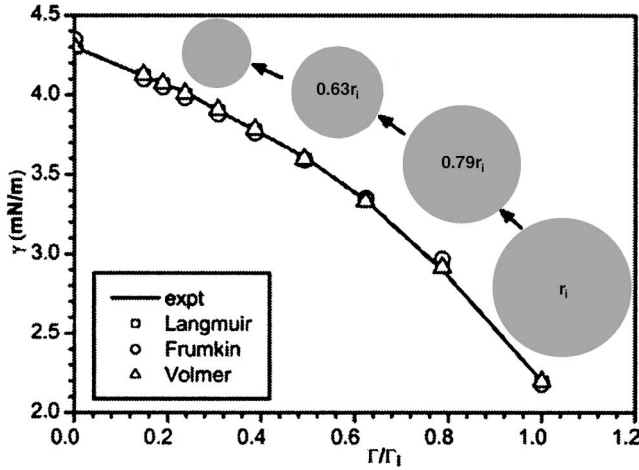


FIG. 1. Measured interfacial tension for a drop and its successive generations of equal size daughter drops created by binary breakups. The ratio of the surface concentration  $\Gamma$  relative to that of the initial drop  $\Gamma_i$  is defined by the change in area at each successive stage of drop breakup. The fits with surface equations are also shown. Viscosity ratio is  $\lambda = 2.3$ .

Langmuir trough experiment. As illustrated in Fig. 1, we first measured  $\sigma$  for a drop with an (unknown) initial surface concentration  $\Gamma_i$  using the small deformation method. Then we broke this drop evenly into two drops and measured  $\sigma$  for the daughter drops. The interfacial tension was checked to be the same for each daughter drop, indicating the surfactants were evenly distributed to both daughter drops. The size of each daughter drop was checked to be equal, which is expected for binary breakup of a drop subjected to our symmetric flow. From mass balance, the surface concentration for the daughter drop was determined to be  $0.79\Gamma_i$ . The daughter drop was then broken up again and the process was repeated many times. In the end, a  $\sigma - \Gamma/\Gamma_i$  isotherm was obtained. To establish a representative surface equation of state for the measured isotherm, we fitted the data to three popular models viz.:

$$\sigma = \sigma_0 + RT\Gamma_\infty \ln(1 - \Gamma/\Gamma_\infty) \text{ (Langmuir),} \quad (1)$$

$$\sigma = \sigma_0 + RT\Gamma_\infty \ln(1 - \Gamma/\Gamma_\infty) + \beta\Gamma^2 \text{ (Frumkin),} \quad (2)$$

$$\sigma = \sigma_0 - RT\Gamma_\infty\Gamma/(\Gamma_\infty - \Gamma) \text{ (Volmar),} \quad (3)$$

where  $\sigma_0$  is the interfacial tension for a clean interface,  $\Gamma_\infty$  is the saturated surfactant surface concentration, and  $\beta$  is a constant to account for the interaction between surfactants. It can be seen that all three models can provide reasonable representation of the data but we use the Langmuir equation due to its good fit and simpler form. This model gives an estimate for  $\Gamma_\infty = 0.38$  chain/nm<sup>2</sup>, which is in the range of measurements (0.1 to 0.5 chain/nm<sup>2</sup>) by other techniques for polymeric surfactants [17,18].

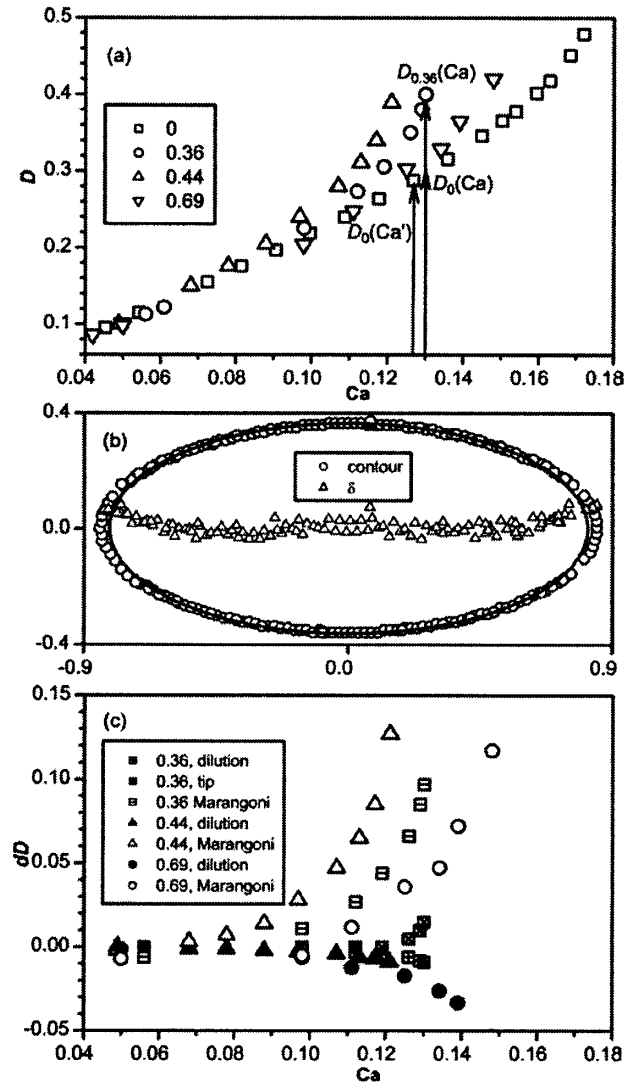


FIG. 2. (a) Steady state drop deformation  $D$  vs capillary number  $Ca$  for  $\lambda = 0.093$  and various surfactant coverage. (b) Drop contour and deviation parameter  $\delta$  in the  $x$ - $y$  plane of a deformed drop with surfactant surface coverage  $\Gamma/\Gamma_\infty = 0.36$  and  $D = 0.40$ . The solid line is a fitted ellipse. (c) Contribution of dilution, tip-stretching, and Marangoni effects to the drop deformation for drops with various surfactant coverage. Tip-stretching is not noticeable and not shown except for  $\Gamma/\Gamma_\infty = 0.36$ .

In the following we discuss the effects of surfactants on steady state drop deformation up to breakup. Figure 2(a) shows this for viscosity ratio  $\lambda = 0.093$  with surfactant coverage estimated from the above Langmuir analysis. For  $D < 0.2$ , surfactants appear to have negligible effects on drop deformation. However, for larger  $D$ , surfactants significantly change deformation relative to that for the clean drop, increasing first for  $\Gamma/\Gamma_\infty$  in the range 0.364 to 0.44 and then decreasing in the range 0.44 to 0.69. A similar trend was predicted by numerical simulation [15] and was observed experimentally by Hu *et al.* [7]. Note

that the initial equilibrium interfacial tension is used to calculate the capillary number so that the simple effect of the reduced  $\sigma$  is already accounted for. The difference between various curves solely represents the collective contribution from the dilution, tip-stretching, and Marangoni effects. Here we shall decompose these effects and quantify each individual contribution.

We use the last data point on the curve with  $\Gamma/\Gamma_\infty = 0.36$  in Fig. 2(a) to illustrate the decomposition procedure. We label it by  $D_{0.36}(\text{Ca})$  for convenience (the subscript represents the surfactant coverage). The coordinates of the data point are  $\text{Ca} = 0.13$  and  $D = 0.40$ . First we investigate the tip-stretching effect by analyzing the contour of the drop in the  $x$ - $y$  plane at that particular deformation by comparing it to an ellipse [Fig. 2(b)]. It has been previously established that the contours of a deformed drop with a clean interface are approximately elliptic for viscosity ratios not much smaller than 0.1 [16]. The elliptic shape can be tested by a deviation parameter  $\delta = x^2/(a/2)^2 + y^2/(b/2)^2 - 1$ , where  $a$  and  $b$  are the axes of the ellipse best fitted to the drop contour. For an ellipse, the deviation parameter is zero everywhere on the contour. If the drop tip is overstretched, the actual drop dimensions  $L$  and  $B$  would be different from  $a$  and  $b$ . The contribution of the tip-stretching to the total drop deformation is then  $dD^{\text{tip}} = (L - B)/(L + B) - (a - b)/(a + b)$ . Figure 2(b) shows that the drop contour near the tip is stretched beyond the elliptic shape and the deviation parameter increases as the contour position approaches the tip. Similar overstressing near the tip is observed for the contour in the  $x$ - $z$  plane (not shown here). The actual dimensions of the drop are measured as  $L = 1.69$ ,  $B = 0.72$ ,  $W = 0.84$  and the axes of the fitted ellipsis  $a$ ,  $b$ , and  $c$  are 1.63, 0.72, 0.84, respectively. The tip-stretching is thus determined to be  $dD^{\text{tip}} = 0.015$ .

Next we calculate the dilution effect. The first step is to calculate the surface area of the deformed drop. We use the surface area equations for ellipsoids since the drop shape only slightly deviates from an ellipsoid, as suggested by the product of the three drop dimensions  $LBW = 1.018$  (a value of unity is expected for a perfect ellipsoid). A surface area of  $4.49\pi$  is thus obtained from the measured drop dimensions. The diluted surface coverage  $\Gamma'/\Gamma_\infty$  after deformation is then  $4\pi/4.49\pi \times 0.364 = 0.324$ . The interfacial tension after dilution  $\gamma' = 3.89$  is calculated from the Langmuir equation and a corrected capillary number  $\text{Ca}' = 0.127$  is finally obtained. The dilution effect  $dD^{\text{dil}}$ , by definition, is the difference between the deformation  $D_0(\text{Ca})$  expected for the uncorrected capillary number  $\text{Ca}$  and the deformation  $D_0(\text{Ca}')$  expected for the capillary number  $\text{Ca}'$  corrected for surface dilution. By interpolation from the  $D_0 - \text{Ca}$  curve,  $D_0(\text{Ca}) = 0.297$  and  $D_0(\text{Ca}') = 0.288$  are obtained, giving a dilution effect of  $D_0(\text{Ca}) - D_0(\text{Ca}') = 0.009$ . The total deformation change due to the surfactant is  $dD = D_{0.36}(\text{Ca}) - D_0(\text{Ca}) = 0.40 - 0.297 = 0.103$ . The

Marangoni effect is thus estimated to be  $dD^m = dD - dD^{\text{dil}} - dD^{\text{tip}} = 0.097$ .

More decomposition results for  $\lambda = 0.093$  are shown in Fig. 2(c). The tip-stretching is significant only for the lowest surfactant coverage  $\Gamma/\Gamma_\infty = 0.36$  and only when the deformation is relatively large ( $D > 0.35$ ). The dilution effect, on the contrary, is small at  $\Gamma/\Gamma_\infty = 0.36$  but becomes larger at larger  $\Gamma/\Gamma_\infty$ . The Marangoni effect is the largest among all the three effects at all surface concentrations. It first increases as  $\Gamma/\Gamma_\infty$  increases from 0.36 to 0.44, but then decreases as  $\Gamma/\Gamma_\infty$  increases further to 0.69. This trend can be explained by the following argument. The Marangoni stresses can be expressed as [15]

$$-\nabla_s \sigma = -\frac{\partial \sigma}{\partial \Gamma} \cdot \nabla_s \Gamma. \quad (4)$$

From Eq. (1) we have

$$\frac{\partial \sigma}{\partial \Gamma} = -\frac{RT}{(1 - \Gamma/\Gamma_\infty)}. \quad (5)$$

Equation (5) indicates that  $\partial \sigma / \partial \Gamma$  increases as  $\Gamma$  increases and approaches  $\Gamma_\infty$ . On the other hand, the concentration gradient  $\nabla_s \Gamma$  decreases with increasing  $\Gamma$ . This is suggested by the fact that tip-stretching, which is indicative of the buildup of the concentration gradient near the tip region, is significant at small surface coverage but disappears at large surface coverage [Fig. 2(c)]. The opposite trends of  $\partial \sigma / \partial \Gamma$  and  $\nabla_s \Gamma$  explain the non-monotonic change of the Marangoni effect, which apparently causes the similar change of the total deformation with the surface coverage in Fig. 2(a).

Figure 3(a) shows the effect of surfactant concentration on the steady state drop deformation for  $\lambda = 2.3$ . The effect of surfactants becomes obvious when  $D$  is larger than about 0.15. Here the deformation is smaller at a given  $\text{Ca}$  for drops with surfactants than that for a clean drop and it decreases monotonically with increasing surface coverage. The individual contribution of different effects can be analyzed in the same fashion as before. Figure 3(b) shows the drop contour in the  $x$ - $y$  plane and fitted ellipse for a deformed drop with  $\Gamma/\Gamma_\infty = 0.74$ ,  $\text{Ca} = 0.108$ , and  $D = 0.4$ . The contour fits the ellipse very well and the deviation parameter fluctuates about zero for every contour point. The contour in the  $x$ - $z$  plane also fits an ellipse (not shown here). The three axes  $a$ ,  $b$ , and  $c$  of the fitted ellipsis are essentially identical to the measured drop dimensions  $L$ ,  $B$ , and  $W$ , which are 1.384, 0.792, and 0.908, respectively, indicating a negligible tip-stretching effect. In fact, for  $\lambda = 2.3$ , no tip-stretching was noticeable at any magnitude of steady state deformation.

The decomposition results for  $\lambda = 2.3$  are shown in Fig. 3(c). In all cases, the dilution effect counts for most

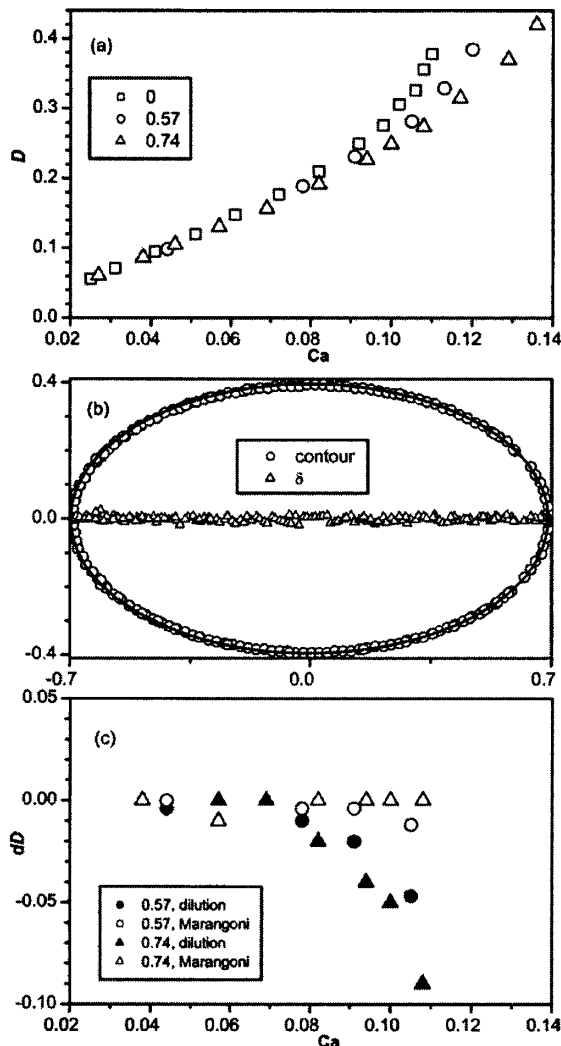


FIG. 3. (a) Steady state drop deformation  $D$  vs capillary number  $Ca$  for  $\lambda = 2.3$  and various surface coverage. (b) Drop contour and deviation parameter  $\delta$  in the  $x$ - $y$  plane of a deformed drop with surface coverage  $\Gamma/\Gamma_\infty = 0.74$  and  $D = 0.42$ . The solid line is a fitted ellipse. (c) Contribution of dilution and Marangoni effects to drop deformation for drops with two different surface coverages. Tip-stretching is not noticeable and thus not shown in the graph.

of the deformation decrease and both the Marangoni and tip-stretching effects are insignificant. The dramatic difference in the Marangoni effect for the two different  $\lambda$ 's may reflect differences in the interfacial retardation num-

ber,  $A = 3\lambda + \text{MaPe}_s$ , where  $\text{Ma} = RT\Gamma_0/\sigma_0 Ca$  is the Marangoni number, and  $\text{Pe}_s = \gamma a^2/D_s$  is the surface Peclet number with  $D_s$  being the surface diffusivity [19]. For both  $\lambda$ 's,  $\text{Ma} = O(1)$  and we estimate  $\text{Pe}_s \gg 1$ . For  $\lambda = 0.093$ , the surfactant significantly slows down the drop interface since  $A$  increases from 0.28 to a value  $\gg 1$ . For  $\lambda = 2.3$ , the interface is already substantially retarded since  $A$  is 6.9 for the clean drop and any further increase in  $A$  results in little change in the drop deformation.

In summary, we have established the surface equation of state and the decomposition of Marangoni, dilution, and tip-stretching effects for polymer drops bearing insoluble surfactant, and we have found a strong influence of viscosity ratio on the balance of these effects.

We thank D. J. Pine, L. G. Leal, and H. A. Stone for helpful discussions.

- 
- [1] G. I. Taylor, Proc. R. Soc. London, Ser. A **146**, 501 (1934).
  - [2] J. M. Rallison, Annu. Rev. Fluid Mech. **16**, 45 (1984).
  - [3] H. A. Stone, Annu. Rev. Fluid Mech. **26**, 65 (1994).
  - [4] R. A. De Bruijn, Chem. Eng. Sci. **48**, 277 (1993).
  - [5] C. D. Eggleton, T. M. Tsai, and K. J. Stebe, Phys. Rev. Lett. **87**, 048302 (2001).
  - [6] R. W. Hooper, V. F. de Almeida, C. W. Macosko, and J. J. Derby, J. Non-Newtonian Fluid Mech. **98**, 141 (2001).
  - [7] Y. T. Hu, D. J. Pine, and L. G. Leal, Phys. Fluids **12**, 484 (2000).
  - [8] J. J. M. Janssen, A. Boon, and W. G. M. Agterof, AIChE J. **40**, 1929 (1994).
  - [9] J. J. M. Janssen, A. Boon, and W. G. M. Agterof, AIChE J. **43**, 1436 (1997).
  - [10] J. Blawdziewicz, V. Cristini, and M. Loewenberg, Phys. Fluids **11**, 251 (1999).
  - [11] X. F. Li and C. Pozrikidis, J. Fluid Mech. **341**, 165 (1997).
  - [12] H. A. Stone and L. G. Leal, J. Fluid Mech. **220**, 161 (1990).
  - [13] W. J. Milliken, H. A. Stone, and L. G. Leal, Phys. Fluids A **5**, 69 (1993).
  - [14] Y. Pawar and K. J. Stebe, Phys. Fluids **8**, 1738 (1996).
  - [15] C. D. Eggleton, Y. P. Pawar, and K. J. Stebe, J. Fluid Mech. **385**, 79 (1999).
  - [16] Y. T. Hu and A. Lips, J. Rheol. **47**, 349 (2003).
  - [17] L. J. Norton *et al.*, Macromolecules **28**, 1999 (1995).
  - [18] J. S. Schulze, B. Moon, T. P. Lodge, and C. W. Macosko, Macromolecules **34**, 200 (2001).
  - [19] J. A. Ramirez and R. H. Davis, AIChE J. **45**, 1355 (1999).